Scattering and lifetime broadening of quantum well states in Pb films on Ag(111)

Michael Becker* and Richard Berndt†
Institut für Experimentelle und Angewandte Physik, Christian-Albrechts-Universität zu Kiel, D-24098 Kiel, Germany
(Received 1 April 2010; published 26 May 2010)

Quantum well states in thin Pb(111) metal films on Ag(111) surfaces were investigated using low-temperature scanning tunneling spectroscopy. Quantitative analysis of the spectra yields the bulk-band dispersion in Γ-L direction, scattering phase shifts at interface and vacuum barrier as well as the lifetime broadening.

DOI: 10.1103/PhysRevB.81.205438 PACS number(s): 68.37.Ef, 72.10.Fk, 73.21.Fg

I. INTRODUCTION

The quantum confinement of electronic states in thin Pb(111) films has attracted considerable interest for almost 40 years.[1,2] When the thickness of a Pb film is reduced to the nanoscale, confinement of electrons results in discrete energy levels associated with so-called quantum well states (QWSs). The specific ratio of interlayer spacing a and Fermi wavelength $\lambda_F(\lambda_F/a \approx 4)$ along the (111) crystallographic direction of Pb causes a modulation of the electron density of states near the Fermi level E_F with bilayer periodicity. Hence, increasing the film thickness by one atomic layer has a significant impact on the physical and chemical properties of the films[3] as shown for, e.g., the electrical resistivity,[4] superconducting transition temperature,[5–7] Hall coefficient,[8] surface energy,[9] work function,[10,11] roughening temperature,[12] step height,[13] electron-phonon coupling,[14] and chemical reactivity.[15] By means of scanning tunneling microscopy (STM) and scanning tunneling spectroscopy (STS) of these quantum well structures it is possible to gain information on the band structure, scattering phase shifts, interface reflectivity, and quasiparticle lifetimes of occupied as well as unoccupied states. The quasiparticle lifetime sets the duration of excitations and, in combination with the group velocity, determines their mean-free path. Excited electrons play an essential role in many physical and chemical surface processes, such as energy transfer, electronically induced adsorbate reactions, catalytic processes, and epitaxy.[16,17] For understanding these surface processes on thin metal films, it is therefore of fundamental importance to study the decay of electronic excitations within these films. Theoretical lifetime studies of Pb films have already been performed for freestanding Pb and for Pb films on Cu(111).[18,19] Experimentally, it has been found that for Pb films on Si(111) the lifetime broadening exhibits a quadratic energy dependence as also found theoretically for freestanding Pb.[18] Contrary to this finding, the theoretical results for Pb/Cu(111) suggest a rather linear dependence of the lifetime broadening on E for energies above E_F+1 eV.[19] However, for Pb on closed-packed noble-metal surfaces, experimental results for the quasiparticle lifetimes are lacking.

Here, we report on a detailed STS study of QWSs in thin Pb(111) films grown on Ag(111) in the thickness range from 1 to 37 monolayers (MLs). From the QWS energies as a function of film thickness, the bulk-band dispersion along Γ-L is derived in the energy region from −0.5 to +3.5 eV around E_F. Simple models of scattering at the two boundaries of the Pb film, i.e., the vacuum barrier and the inverted sp-band gap of the Ag(111) interface yield a rather accurate description of the energy dependence of the scattering phase shift Φ.[20] Moreover, the widths of the spectroscopic features of the QWS are analyzed, giving insight into hot-electron and hot-hole dynamics in Pb films on Ag(111).

II. EXPERIMENT

Measurements were performed with a home-built scanning tunneling microscope operated at 5 K in ultrahigh vacuum conditions. The tunneling voltage is applied to the sample. Ag(111) single-crystal surfaces were prepared by repeated Ar^+ sputter/anneal cycles. Pb islands of several ML thickness were obtained by room-temperature deposition from a tungsten crucible with a deposition rate of 1 ML/min. Pb grows on Ag(111) in the Stranski-Krastanov mode[21,22] with an initial 1-ML-thick wetting layer (WL). At higher coverage, flat-top islands of distinct heights are formed. Film thicknesses are numbered in ML including the WL. Electrochemically etched W tips were prepared by annealing cycles and indenting into Pb islands, thereby covering the tip apex with Pb. Spectra of the differential conductance (dI/dV) were acquired by using standard lock-in detection (modulation amplitude 2.5 mV_{rms}, frequency 10 kHz).

III. MODELING

For our study we utilize the phase accumulation model (PAM) (Refs. 23 and 24) which has been very successful in the interpretation of image and surface states on clean metals and of QWSs in layered noble-metal systems.[25] The quantization condition for the existence of such states is based on the Bohr-Sommerfeld quantization rule

$$2k(E)(d+d_0)+\Phi = 2\pi n, \tag{1}$$

where $\Phi=\Phi_C+\Phi_B$ is the sum of the phase shifts on reflection at the crystal Φ_C and at the vacuum barrier Φ_B, and $k(E)$ is the energy dependent wave vector of an electron propagating along the Γ-L direction of Pb in a slab of thickness $d+d_0$. $d=aN$ is the nominal thickness, with N the number of atomic layers, and $a=2.86$ Å. d_0 is a constant offset which accounts for the displacement of the position of the Pb/Ag interface and of the image plane with respect to the jellium edges of the film due to the spill out of electrons on both sides of the slab.[3] We assume d_0 to be independent of N and use it as a fit parameter. For constructive interference the

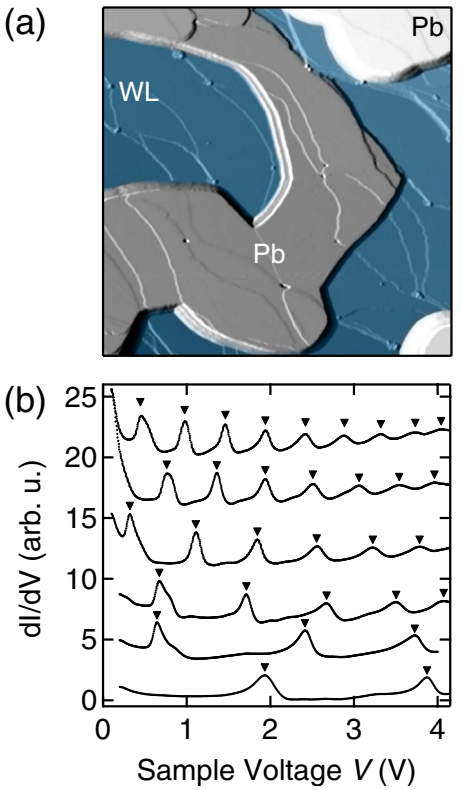

FIG. 1. (Color online) (a) Processed image of Pb islands on Ag(111) (600×600 nm^2, $V=0.2$ V). Ag steps are clearly "shining through" the Pb island. (b) Representative constant-current dI/dV spectra acquired on Pb islands with film thicknesses of 3, 6, 12, 17, 22, and 27 ML from bottom to top, respectively ($I=5$ nA). Triangles indicate the extracted QWS energy. Spectra are vertically shifted for clarity.

total phase accumulation must be an integer multiple of 2π. The integer quantum number n corresponds to the number of half wavelengths of the wave function inside the slab. For Φ_B we have used the WKB expression,[26]

$$\Phi_B = \pi[3.4\ \text{(eV)}/(E_V - E)]^{1/2} - \pi \tag{2}$$

with E_V the vacuum level. E_V has been shown to vary with bilayer periodicity.[10,11] Here we fix a single value for all layer thicknesses and use E_V as a fit parameter.

The interface phase shift Φ_C should vary from 0 to π across the inverted sp-band gap of Ag(111), varying rapidly with E at the band edges.[24,27] We have used the empirical expression,[20,28]

$$\Phi_C = 2\ \arcsin[(E - E_L)/(E_U - E_L)]^{1/2}, \tag{3}$$

where E_U and E_L are the energies of the upper and lower edges of the projected band gap in Ag(111), respectively. Here $E_L=-0.4$ and $E_U=3.9$ eV.[29] Throughout this paper energies are measured with respect to the Fermi level of the sample.

IV. RESULTS AND DISCUSSION

Figure 1(a) shows an image of Pb islands protruding from the WL of Pb/Ag(111). On Pb islands, which extend over several adjacent Ag terraces, the difference in interlayer spacing between Pb (2.86 Å) and Ag (2.36 Å) causes a dislocation running from the Pb/Ag interface to the surface. This produces a step of 0.5 Å height at the island surface. These dislocation lines are clearly visible in the shown image, Fig. 1(a), and are used to discriminate different island thicknesses. The image has been processed to enhance the contrast of steps and dislocation lines.

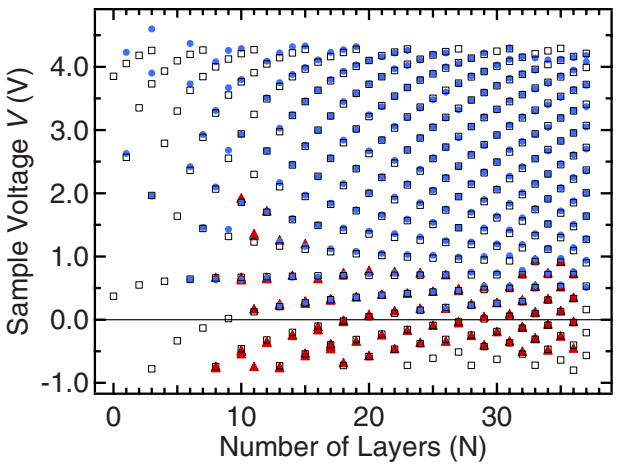

FIG. 2. (Color online) QWS energies versus island height for Pb on Ag(111) numbered in monatomic layers. Dots and triangles are obtained from constant-current and constant-height dI/dV, respectively. Open squares show calculated QWS energies as described in the text ($v_g=13.19$ eV Å, $k_F=1.592$ Å^{-1}, $d_0=-0.18$ Å, and $E_V=4.5$ eV).

A collection of representative constant-current dI/dV spectra acquired atop of various island heights is displayed in Fig. 1(b). The spectra show a number of unoccupied states. Similar spectra have been found in Pb islands on Cu(111).[30] The peak positions correspond to the extracted QWS energies of each island and are highlighted by solid triangles [Fig. 1(b)]. For sample voltages $V<1$ V, the peak structure displays a shoulder toward higher voltages. For $V>1$ V the peaks become more symmetric. This is due to the specific band structure of thin Pb films.[31] In constant-height dI/dV spectra the states at $V<1$ V exhibit box-shaped line shapes with an arctanlike onset as will be discussed in more detail in Sec. IV B (see also Fig. 5).

Figure 2 shows the layer resolved QWS energies versus island height for Pb/Ag(111) numbered in monatomic layers. Dots and triangles are obtained from constant-current [cf. Fig. 1(b)] and constant-height dI/dV, respectively. Open squares show QWS energies calculated as described in the following. Similar to Pb adsorbed on Cu(111) and Si(111) some island heights—2, 4, 5, 7, and 9 ML in the present case—are hardly observed.[32–34] For $V<1$ V, the QWS energies are determined from the constant-height data as the midpoint of the onset of the arctanlike spectral feature.[35] For $V>1$ V the peak position of the Lorentzian-type line shapes is used.

The sections below are organized as follows. In Sec. IV A, the bulk dispersion along Γ-L is derived and the scattering phase shifts are analyzed. In Sec. IV B, we analyze the onset widths of the spectroscopic signals of the QWSs, giv-

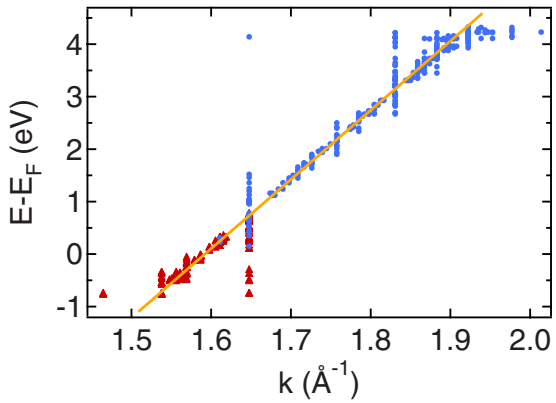

FIG. 3. (Color online) Bulk band dispersion along the Γ-L direction shown in the extended Brillouin-zone scheme. Data from constant-current and constant-height data are indicated by dots and triangles, respectively. A linear fit (solid line) yields v_g=13.19 eV Å and k_F=1.592 Å^{-1}.

ing insight into hot-electron and hot-hole dynamics in the Pb films.

A. Electronic structure

From the energies of the QWSs as a function of film thickness, the bulk-band dispersion along the Γ-L direction can be derived. Figure 2 displays the layer resolved QWS energies. For the determination of the quantum number n of each QWS, we utilize the fact that the energy of the particular QWS located at ≈0.65 eV on islands consisting of an even number of Pb layers is rather independent of the slab thickness. It has been shown that the wave vector k of this state is $3\pi/2a$.[36] Hence, the corresponding quantum number n for all QWSs shown in Fig. 2 (dots and triangles) can be derived.[30]

The sum of the thickness-independent phase shifts $\Phi_{t\text{-}i}=\Phi_C+\Phi_B+2k(E)d_0$ depends only on the electron energy. Hence, the wave vector $k(E)$ at a given energy can be derived from the QWSs at that energy. Consider N_1 and N_2, corresponding to film thicknesses of two QWSs at the same energy $E=E_1=E_2$ with quantum number n_1 and n_2, respectively. Equation (1) leads to

$$k(E) = \pi(n_2 - n_1)/[(N_2 - N_1)a]. \quad (4)$$

In view of the uncertainty margins in determining QWS energies from dI/dV spectra, we applied Eq. (4) to pairs of QWSs whose energies differ by less than 30 meV, i.e., $|E_2-E_1|\leq 30$ meV. Figure 3 summarizes the results for the dispersion along Γ-L in an extended Brillouin-zone scheme. The band exhibits an approximately linear relation between E and k over the entire energy range.[37] The slope of the dispersion relation converts to a constant group velocity v_g =13.19 eV Å and a Fermi wave vector k_F=1.592 Å^{-1}. The result for k_F is very close to the value from angle-resolved photoemission spectroscopy, k_F=1.598 Å^{-1}, and de Haas-van Alphen measurements, k_F=1.596 Å^{-1}.[14,38,39] It is important to note that the dispersion relation of Fig. 3 has been obtained without using the scattering phase shift at the vacuum barrier. Thus, our result would not be affected by a STM-induced Stark shift.[40]

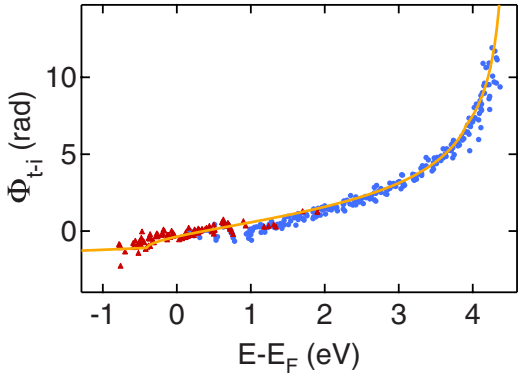

FIG. 4. (Color online) $\Phi_{t\text{-}i}$, sum of the thickness-independent phase shifts. Data from constant-current and constant-height data are indicated by dots and triangles, respectively. $\Phi_{t\text{-}i}$ as calculated from Eqs. (1)–(3) with v_g=13.19 eV Å, k_F=1.592 Å^{-1}, d_0=−0.18 Å, and E_V=4.5 eV is shown as a solid line.

Using the above derived linear dispersion relation along Γ-L, we can now calculate the scattering phase shifts from the experimental data. Figure 4 shows the resulting $\Phi_{t\text{-}i}$ (dots and triangles). A solid line shows $\Phi_{t\text{-}i}$ as calculated from Eqs. (1)–(3). Given the expressions for Φ_B and Φ_C we find that the experimental data are best described with d_0=−0.18 Å and E_V=4.5 eV. Figure 4 shows that simple models for the scattering phase shift yield a rather accurate description for the experimentally observed $\Phi_{t\text{-}i}$ over the entire energy range investigated here. The divergence of Φ_B for $E\rightarrow E_V$ is clearly observable and points to the massive impact of the vacuum barrier phase shift on the energetic positions of the higher lying QWSs. E_V=4.5 eV as found here compares well with E_V=4.6 eV as inferred from STS data of Pb QWSs on Cu(111).[30] Furthermore, the very good agreement of calculated QWS energies, using the PAM together with the

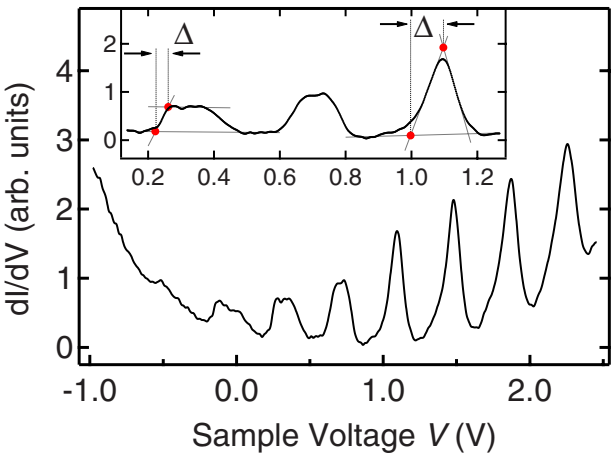

FIG. 5. (Color online) Exemplary constant-height dI/dV spectrum of 36 ML Pb. Inset shows a zoom in the same spectrum. The three gray lines on the left and on the right QWS indicate how the onset linewidths are determined for arctanlike QWS line shapes (left) and a Lorentzian-type line shape (right). Red dots highlight the intersection points, used to determine Δ.

derived values for v_g=13.19 eV Å, k_F=1.592 Å^{-1}, d_0=−0.18 Å, and E_V=4.5 eV, and the experimental data as shown in Fig. 2 are remarkable.

B. Lifetime broadening

In the following, we discuss the linewidths of the Pb/Ag(111) QWSs. Figure 5 shows an exemplary constant-height dI/dV spectrum of an 36 ML Pb film. The shapes of the QWS features change with varying voltage. For $V<1$ V the QWSs give rise to box-shaped spectral features, while for $V>1$ V the line shapes are Lorentzian type. We found that this energy dependence of the spectral line shapes is universal for all investigated film thicknesses and we assign it to the peculiar band structure of the Pb QWSs.

For Pb films it has been shown that the dispersion of the QWSs shows a quasifree-electronlike dispersion near the zone center $\bar{\Gamma}$ but at larger in-plane momenta the dispersion flattens.[31,41–43] For QWSs at higher energies, the effective mass near $\bar{\Gamma}$ increases. For the unoccupied QWSs in the vicinity of $\bar{\Gamma}$, this can result in almost nondispersive bands, yielding a Lorentzian line shape in STS.[44–46] Hence, for voltages below 0.9 eV we assume that the onset is well described by the arctan-shaped onset of a two-dimensional quasifree electron gas.[35] The steplike spectral features of the QWSs are in contrast to spectra measured on Pb/Si(111) where also the QWS below 1 V exhibit Lorentzian line shapes.[10,18] This difference in line shape may be explained by the enhanced lossy interface scattering, induced by disorder at the Pb/Si interface as observed in Ref. 18, affecting the line shape of the QWSs. Therefore, from observing the arctan-shaped onsets we infer that Pb films on Ag(111) exhibit a high-quality ordered interface.

As for QWSs with energies above 1 eV the observed spectral feature turns to a symmetric Lorentzian line shape, the contribution of tunneling electrons with finite in-plane momenta decreases and should contribute less than 10 meV to the Lorentzian linewidth of the excitation at the $\bar{\Gamma}$ point.[44,45] Hence, we assign Lorentzian line shapes to QWSs with energies above 1.1 eV. For QWSs with energies ranging from 0.9 to 1.1 eV the distinction between arctan and Lorentzian line shape is difficult and therefore we concentrate on QWS energies outside this energy range. In order to determine the lifetime broadening we analyze the QWSs onset widths following the surface-state analysis of Li *et al.* described in Ref. 35. To quantify the onset width, which we denote Δ, we adopt the geometrical definition illustrated in the inset in Fig. 5. For arctanlike features (left QWS) we extrapolate the slope at the midpoint of the rise to the continuation of the differential conductance above and below the onset. For Lorentzian-type features (right QWS) we extrapolate the slope at the steepest point of the rise to the continuation of the differential conductance below the onset and to the continuation of the steepest point of the trailing edge. The red dots highlight the intersection points, used to determine Δ.

We have also used constant-current dI/dV spectra to determine Δ. In order to minimize the distorting influence of the constant-current modus on the observed line shapes we normalize the constant-current dI/dV spectra to remove the influence of the changing tip-sample distance.[47–49] We find that the normalization recovers the box-shaped QWS spectra for energies below 1 eV. For the unoccupied states we find that analyzing the two kinds of dI/dV spectra, i.e., constant height and normalized constant current, yield linewidths which are in good agreement. This indicates the reliability of the normalization scheme also for linewidth determinations in the shown voltage range.

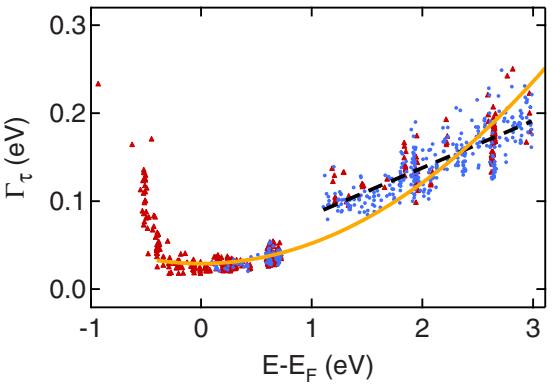

FIG. 6. (Color online) Lifetime broadening Γ_τ. Data from constant-current and constant-height data are indicated by dots and triangles, respectively. Solid orange line is a quadratic fit to the energy range from $E-E_F$=−0.4 to 3 eV. A dashed black line shows a linear fit for $E-E_F>1$ eV.

For arctan line shapes, the lifetime broadening Γ_τ can be extracted from the geometrical onset width Δ as $\Gamma_\tau=(2/\pi)\Delta$.[17,35] For Lorentzian line shapes it can be shown by means of simple line shape analysis arguments that the geometrical onset width Δ as defined above relates to Γ_τ as $\Gamma_\tau=(2/\sqrt{3})\Delta$.

Figure 6 shows Γ_τ, obtained using the above-mentioned line shape analysis. We find that for energies below $E\approx-0.4$ eV, Γ_τ increases more rapidly as a function of $|E|$ than for positive voltages. We assign this to the lower band edge in Ag(111). Below the lower band edge at $E=-0.4$ eV the Pb QWSs turn into quantum well resonances due to the reduced confinement at the Pb/Ag interface. Thus, the elastic-scattering rate of holelike excitations in the quantum well rises, leading to the observed increase in Γ_τ.[19,50] For energies within the inverted *sp*-band gap (−0.4 eV$<E<$3.9 eV), we find that Γ_τ is independent of film thickness within the uncertainty margins. Hence, we assume the linewidth contribution due to the lossy interface scattering into the Ag(111) substrate to be rather small.

In the absence of defects within the Pb films, there are mainly three contributions to Γ_τ to be considered,

$$\Gamma_\tau=\Gamma_0+\Gamma_{e\text{-}p}(E)+\Gamma_{e\text{-}e}(E). \quad (5)$$

$\Gamma_{e\text{-}e}(E)$ and $\Gamma_{e\text{-}p}(E)$ denote the electron-electron (e-e) and electron-phonon-scattering rates, respectively. Γ_0 accounts for the lossy interface scattering. In Ref. 18, $\Gamma_{e\text{-}p}(E)\approx20$ meV at E_F has been calculated for freestanding Pb at a temperature of 5 K. As $|\Gamma_{e\text{-}p}(E_F)-\Gamma_{e\text{-}p}(E)|<10$ meV for E

≤ 2.5 eV, we assume a constant contribution of $\Gamma_{e\text{-}p}$ to the lifetime broadening over the energy range investigated here. From Fermi-liquid theory, as shown by Quinn-Ferrell, the e-e scattering is expected to exhibit a quadratic energy dependence for states close to E_F.[51] For Pb such a description yields $\Gamma_{e\text{-}e}(E)=\alpha(E-E_F)^2$ with $\alpha=0.027$ eV^{-1}. The solid orange line shows such a quadratic energy dependence fitted to our data in the energy range between −0.4 and 3 eV. The jump in Γ_τ that occurs at $E\approx 1$ eV is linked to the different line shapes found for QWSs with energies below and above ≈ 1 eV. For the e-e scattering we find $\alpha=0.023$ eV^{-1} which compares very well with the Quinn-Ferrell value and with $\alpha=0.026$ eV^{-1} as measured by Hong *et al.*[18] However, for energies above 1 eV a deviation of the quadratic energy dependence (shown by the dashed black line in Fig. 6) is observed. The fitted line has a slope of 53 meV eV^{-1}. A similar linear dependence has also been found theoretically for Pb islands on Cu(111).[19] There it has been argued that the linear dependence is signaling deviations of the random-phase-approximation linewidth from simple quadratic dependence. The reported slope of 52 meV eV^{-1} is in good agreement with our measured data.

The fit also yields a constant offset of $\Gamma_0+\Gamma_{e\text{-}p}(E_F)=29$ meV. Comparing this result with the above-mentioned calculations for $\Gamma_{e\text{-}p}$ of freestanding Pb, supports the assumption that the contribution of the lossy scattering to the lifetime broadening is small and on the order of $\Gamma_0\approx 10$ meV at E_F. A similar analysis for the $\sqrt{3}\times\sqrt{3}$ and the 7×7 interface of Pb/Si yields $\Gamma_0\approx 50$ meV and ≈ 140 meV at E_F, respectively.[18] Hence, the Pb/Ag interface yields a better confinement than the Pb/Si interface and this possibly causes the observability of the box-shaped QWSs below ≈ 1 eV.

V. CONCLUSION

In summary, quantum well states in Pb(111) films up to 37 ML have been investigated. The thickness dependence of the QWS energies is found to be very well fitted with the phase accumulation model including energy-dependent scattering phase shifts at the interface and the vacuum barriers. The dispersion along the Γ-L direction is well approximated by a constant group velocity of $v_g=13.19$ eV Å. The Pb/Ag interface is of high quality, such that the lossy interface scattering contribution to the lifetime broadening is significantly reduced compared to Pb/Si interfaces. The electron-electron lifetime broadening follows to a good approximation a quadratic energy dependence $\Gamma_{e\text{-}e}=\alpha(E-E_F)^2$ with $\alpha=0.023$ eV^{-1}. However small deviations of the quadratic energy dependence are observed and may be caused by a deviation of the screening behavior of the Pb electrons compared to that of a homogeneous electron gas.[19]

ACKNOWLEDGMENT

Financial support by the Innovationsfonds Schleswig-Holstein is gratefully acknowledged.

*becker@physik.uni-kiel.de
†berndt@physik.uni-kiel.de

[1] R. C. Jaklevic, J. Lambe, M. Mikkor, and W. C. Vassell, Phys. Rev. Lett. **26**, 88 (1971).
[2] S. Qin, J. Kim, Q. Niu, and C. Shih, Science **324**, 1314 (2009).
[3] F. Schulte, Surf. Sci. **55**, 427 (1976).
[4] R. C. Jaklevic and J. Lambe, Phys. Rev. B **12**, 4146 (1975).
[5] Y. Guo *et al.*, Science **306**, 1915 (2004).
[6] C. Brun, I. P. Hong, F. Pattney, I. Y. Sklyadneva, R. Heid, P. M. Echenique, K. P. Bohnen, E. V. Chulkov, and W. D. Schneider, Phys. Rev. Lett. **102**, 207002 (2009).
[7] T. Zhang, P. Cheng, W. J. Li, Y. J. Sun, G. Wang, X. G. Zhu, K. He, L. Wang, X. Ma, X. Chen, Y. Wang, Y. Liu, X. Q. Lin, J. F. Jia, and Q. K. Xue, Nat. Phys. **6**, 104 (2010).
[8] M. Jałochowski, M. Hoffman, and E. Bauer, Phys. Rev. Lett. **76**, 4227 (1996).
[9] C. M. Wei and M. Y. Chou, Phys. Rev. B **66**, 233408 (2002).
[10] Y. Qi, X. Ma, P. Jiang, S. Ji, Y. Fu, J. Jia, Q. Xue, and S. B. Zhang, Appl. Phys. Lett. **90**, 013109 (2007).
[11] M. Becker and R. Berndt, Appl. Phys. Lett. **96**, 033112 (2010).
[12] F. Calleja, M. C. G. Passeggi, Jr., J. J. Hinarejos, A. L. Vázquez de Parga, and R. Miranda, Phys. Rev. Lett. **97**, 186104 (2006).
[13] A. Crottini, D. Cvetko, L. Floreano, R. Gotter, A. Morgante, and F. Tommasini, Phys. Rev. Lett. **79**, 1527 (1997).
[14] Y. F. Zhang, J. F. Jia, T. Z. Han, Z. Tang, Q. T. Shen, Y. Guo, Z. Q. Qiu, and Q. K. Xue, Phys. Rev. Lett. **95**, 096802 (2005).
[15] X. Ma, P. Jiang, Y. Qi, J. Jia, Y. Yang, W. Duan, W. Li, X. Bao, S. B. Zhang, and Q. Xue, Proc. Natl. Acad. Sci. U.S.A. **104**, 9204 (2007).
[16] H. Nienhaus, Surf. Sci. Rep. **45**, 1 (2002).
[17] P. M. Echenique, R. Berndt, E. V. Chulkov, T. Fauster, A. Goldmann, and U. Höfer, Surf. Sci. Rep. **52**, 219 (2004).
[18] I. P. Hong, C. Brun, F. Patthey, I. Y. Sklyadneva, X. Zubizarreta, R. Heid, V. M. Silkin, P. M. Echenique, K. P. Bohnen, E. V. Chulkov, and W. D. Schneider, Phys. Rev. B **80**, 081409(R) (2009).
[19] A. Zugarramurdi, N. Zabala, V. M. Silkin, A. G. Borisov, and E. V. Chulkov, Phys. Rev. B **80**, 115425 (2009).
[20] N. V. Smith, N. B. Brookes, Y. Chang, and P. D. Johnson, Phys. Rev. B **49**, 332 (1994).
[21] K. Takayanagi, D. Kolb, K. Kambe, and G. Lehmpfuhl, Surf. Sci. **100**, 407 (1980).
[22] A. Rolland, J. Bernardini, and M. Barthes-Labrousse, Surf. Sci. **143**, 579 (1984).
[23] P. M. Echenique and J. B. Pendry, J. Phys. C **11**, 2065 (1978).
[24] N. V. Smith, Phys. Rev. B **32**, 3549 (1985).
[25] D. Luh, T. Miller, J. J. Paggel, M. Y. Chou, and T. Chiang, Science **292**, 1131 (2001).
[26] E. McRae and M. Kane, Surf. Sci. **108**, 435 (1981).
[27] D. P. Woodruff, W. A. Royer, and N. V. Smith, Phys. Rev. B **34**, 764 (1986).
[28] P. Echenique and J. Pendry, Prog. Surf. Sci. **32**, 111 (1989).
[29] E. V. Chulkov, V. M. Silkin, and P. M. Echenique, Surf. Sci. **437**, 330 (1999).

[30] M. C. Yang, C. L. Lin, W. B. Su, S. P. Lin, S. M. Lu, H. Y. Lin, C. S. Chang, W. K. Hsu, and T. T. Tsong, Phys. Rev. Lett. **102**, 196102 (2009).
[31] M. H. Upton, T. Miller, and T. C. Chiang, Phys. Rev. B **71**, 033403 (2005).
[32] R. Otero, A. L. Vázquez de Parga, and R. Miranda, Phys. Rev. B **66**, 115401 (2002).
[33] R. Otero, A. L. Vázquez de Parga, and R. Miranda, Surf. Sci. **447**, 143 (2000).
[34] M. Hupalo and M. C. Tringides, Phys. Rev. B **65**, 115406 (2002).
[35] J. Li, W. D. Schneider, R. Berndt, O. R. Bryant, and S. Crampin, Phys. Rev. Lett. **81**, 4464 (1998).
[36] W. B. Su, S. H. Chang, W. B. Jian, C. S. Chang, L. J. Chen, and T. T. Tsong, Phys. Rev. Lett. **86**, 5116 (2001).
[37] The piling up of data points around $k=3\pi/2a=1.648$ Å^{-1} and $k=5\pi/3a=1.831$ Å^{-1} is due to the finite-energy window of 30 meV used to determine $k(E)$. The piling can be removed by reducing the energy window. However, the resulting slope of the dispersion is not affected when changing the energy window to 3 meV.
[38] J. R. Anderson and A. V. Gold, Phys. Rev. **139**, A1459 (1965).
[39] M. Jałochowski, H. Knoppe, G. Lilienkamp, and E. Bauer, Phys. Rev. B **46**, 4693 (1992).
[40] L. Limot, T. Maroutian, P. Johansson, and R. Berndt, Phys. Rev. Lett. **91**, 196801 (2003).
[41] J. H. Dil, J. W. Kim, Th. Kampen, K. Horn, and A. R. H. F. Ettema, Phys. Rev. B **73**, 161308(R) (2006).
[42] F. Yndurain and M. P. Jigato, Phys. Rev. Lett. **100**, 205501 (2008).
[43] N. Miyata, K. Horikoshi, T. Hirahara, S. Hasegawa, C. M. Wei, and I. Matsuda, Phys. Rev. B **78**, 245405 (2008).
[44] A. Bauer, A. Mühlig, D. Wegner, and G. Kaindl, Phys. Rev. B **65**, 075421 (2002).
[45] D. Wegner, A. Bauer, and G. Kaindl, Phys. Rev. Lett. **94**, 126804 (2005).
[46] D. Wegner, A. Bauer, Y. M. Koroteev, G. Bihlmayer, E. V. Chulkov, P. M. Echenique, and G. Kaindl, Phys. Rev. B **73**, 115403 (2006).
[47] To obtain the normalized differential conductance dI/dV_N, the dI/dV signal is divided by the transmission factor $T(V,\bar{z})=\exp[-\bar{z}\sqrt{8m/\hbar^2(E_V-eV/2)}]$ of electrons emanating from the Fermi level of the tip. Here, $\hbar$ is the reduced Planck constant, m the electron mass, and $-e$ the electron charge. We used $E_V=4.5$ eV and $\bar{z}$ is calculated as $\bar{z}(V)=z(V)+5$ Å, where $z(V)$ is the constant-current vertical tip displacement measured concomitantly with dI/dV.
[48] J. Li, W. D. Schneider, and R. Berndt, Phys. Rev. B **56**, 7656 (1997).
[49] M. Ziegler, N. Neel, A. Sperl, J. Kröger, and R. Berndt, Phys. Rev. B **80**, 125402 (2009).
[50] T. Miller, A. Samsavar, G. E. Franklin, and T. C. Chiang, Phys. Rev. Lett. **61**, 1404 (1988).
[51] J. J. Quinn and R. A. Ferrell, Phys. Rev. **112**, 812 (1958).